sustainability

MDPI

Article

The Utilization of Waste Marble Dust as a Cement Replacement in Air-Cured Mortar

Nadhir Toubal Seghir [1], Mekki Mellas [1], Łukasz Sadowski [2,*], Aleksandra Krolicka [3], Andrzej Żak [3] and Krzysztof Ostrowski [4]

1 Civil Engineering Research Laboratory, Biskra University, Biskra 07000, Algeria; tsnadhir@gmail.com (N.T.S.); m.mellas@univ-biskra.dz (M.M.)
2 Faculty of Civil Engineering, Wroclaw University of Technology, Wybrzeze Wyspianskiego 27, 50-370 Wroclaw, Poland
3 Faculty of Mechanical Engineering, Wroclaw University of Technology, Wybrzeze Wyspianskiego 27, 50-370 Wroclaw, Poland; aleksandra.krolicka@pwr.edu.pl (A.K.); andrzej.zak@pwr.edu.pl (A.Ż.)
4 Institute of Building Materials and Structures, Cracow University of Technology, 24, Warszawska Str., 31-155 Cracow, Poland; krzysztof.ostrowski.1@pk.edu.pl
* Correspondence: lukasz.sadowski@pwr.edu.pl; Tel.: +48-71-320-37-42

Received: 5 March 2019; Accepted: 9 April 2019; Published: 12 April 2019

Abstract: The aim of this study is to assess the possibility of utilizing waste marble dust (WMD) as a partial cement substitution in air-cured mortar (ACM). Three different levels of cement replacement were analyzed: 5%, 10% and 15% by cement weight. The specimens were manufactured in a local laboratory at an air temperature of 22 ± 2 °C and a humidity equal to 20 ± 1%. The chemical and physical properties of ordinary Portland cement and WMD has been found to be the most crucial parameters. A variety of macroscopic tests, such as apparent density, porosity and compressive strength, were proposed in order to explain the effect of utilizing the WMD on the ACM. To confirm the results of the macroscopic properties, thorough microstructural analysis using scanning electron microscopy (SEM) was performed. The obtained results of this study indicate that replacing cement with WMD affects the physical and mechanical properties of air-cured mortar. The apparent density and compressive strength decrease while the porosity increases.

Keywords: air-cured mortar; waste marble dust; compressive strength; porosity

1. Introduction

The leading factor influencing the quality of cement-based composites and their appropriate adherence is ordinary Portland cement. The manufacturing of ordinary Portland cement requires a meaningful consumption of energy [1,2] and the production of enormous greenhouse gas emissions, including carbon monoxide (CO), carbon dioxide (CO_2), nitrogen oxides (NOx), black carbon (BC), and sulfur dioxide (SO_2) [3], therefore contributing to environmental pollution [4,5]. Global cement production (4.18 billion tones in 2014) is the third biggest source of carbon dioxide emissions [6]. The average value of CO_2 intensity emissions from all worldwide cement production is 222 kg of CO_2/t of cement [7].

From an economic point of view, it can be seen to be reasonable to replace a part of ordinary Portland cement with waste mineral dust. In addition, this treatment is an environmentally friendly solution [8–10]. Due to an excessive amount of very fine particles in dust, the voids in cement-based materials could be thoroughly filled. The particle size and chemical composition of this by-product allow this material to be treated as an attractive additive in cement-based material technology [11].

Marble has been widely used as a building material in the civil engineering industry [12]. During the mining process and in the polishing of marble stone, marble dust is perceived as a waste material [13].

These by-products are present in the environment and contribute to pollution [14,15]. The utilization of marble dust reduces the cost of cement-based material production and also decreases the costs of removing it from the environment [16].

The possibility of using waste materials such as marble dust as a partial substitution in the production of mortar and concrete has often been investigated by researchers [5,17–29]. Its mechanical properties are the main aspect of the analysis. Consequently, it has been proved that the utilization of waste marble dust (WMD) in cement mortar improves its mechanical and physical properties when subjected to the water-curing condition [10]. The author's previous study showed that the water-curing condition, when compared to the air-curing condition, was profitable for the acceleration of the hydration rate of cement-based materials blended with WMD dust [30]. However, on real construction sites, cement-based materials are mainly prepared and stored in air conditions (in nature) [10].

Based on the performed literature review, there is no study related to the properties of air-cured mortar containing WMD. To fill this knowledge gap, this research studies the effect of the partial replacement of ordinary Portland cement with WMD on the macro and micro properties of mortars stored at an air temperature equal to 22 ± 2 °C and a relative humidity of 20 ± 1% by determining the compressive strength and apparent density. In addition, scanning electron microscopy (SEM) analysis was also performed to determine the porosity and Si/Ca ratios of ACM after 28 days of being cured.

2. Materials and Methods

2.1. Materials

The following materials were used to manufacture the mortars: ordinary Portland cement CEM I 42.5 R, produced by Biskria ciment, containing 95% clinker with 5% gypsum for the setting regulation. As the partial ordinary Portland cement replacement, waste marble from the aggregate production of marble stone in the CHATT/FilFila quarry of the Skikda region was used. Before use, it was ground to the proper size in order to obtain a WMD fineness in the ordinary Portland cement fineness range (between 3000 to 4000 cm^2/g) [30].

Sand from the Biskra region (Oued-Djedi River) with a particle size between 0 and 5 mm was used as fine aggregate. It was first cleaned and fractionated with the use of a sieving machine to receive a 0/2 particle size (Figure 1) according to the standard EN 196-1 [31]. Tap water was used in the manufacturing of the mortars.

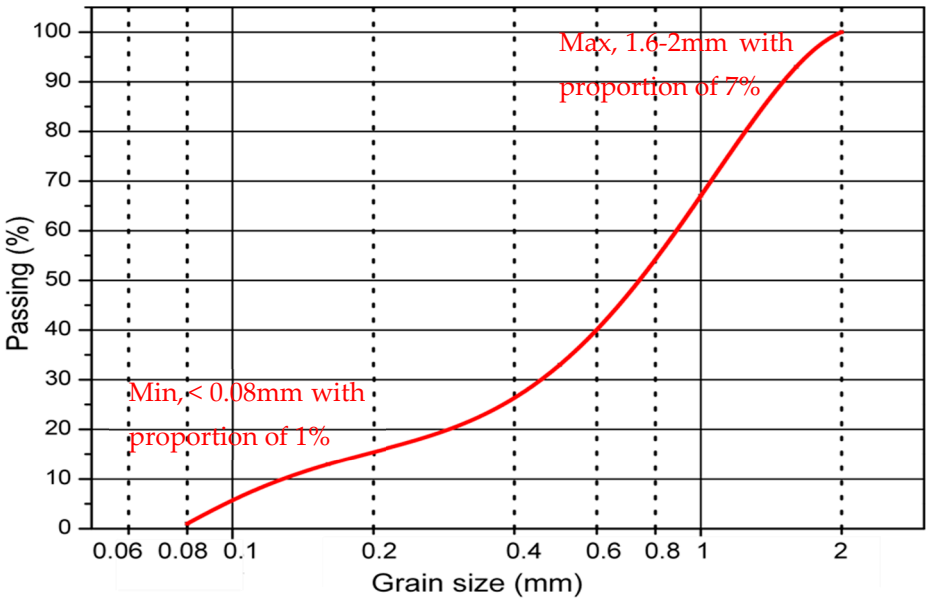

Figure 1. Particle size distribution curve (PSD) of reconstituted river cleaner sand (0/2 mm).

Table 1 presents the mineralogical and chemical composition, as well as the physical properties of the ordinary Portland cement, WMD and sand used in the study. Figure 2 presents the X-ray diffraction (XRD) spectrum of these materials.

Table 1. Properties of the ordinary Portland cement, WMD and sand [10].

Oxide Content (%)	Ordinary Portland Cement	WMD	Sand
SiO_2	20.83	0.05	58.15
Al_2O_3	4.13	0.05	0.34
Fe_2O_3	5.58	0.02	0.65
CaO	62.91	56.94	22.08
MgO	1.42	0.92	0.28
SO_3	2.30	0.32	0.018
K2O	0.38	0.009	0.00
Cl	0.028	0.001	0.018
Loss on ignition (L.O.I)	2.04	41.63	18.23
Insoluble Residue (I.R)	0.382	0.06	0.234
Mineralogical composition			
C_3S	62.03	-	
C_2S	13	-	
C_3A	1.5	-	
C_4AF	16.98	-	
Physical properties			
Solid density (kg/m^3)	3150	2740	2656.5
Bulk density (kg/m^3)	980	980	1631.23
Blaine fineness (cm^2/g)	3571.78	3869.46	-

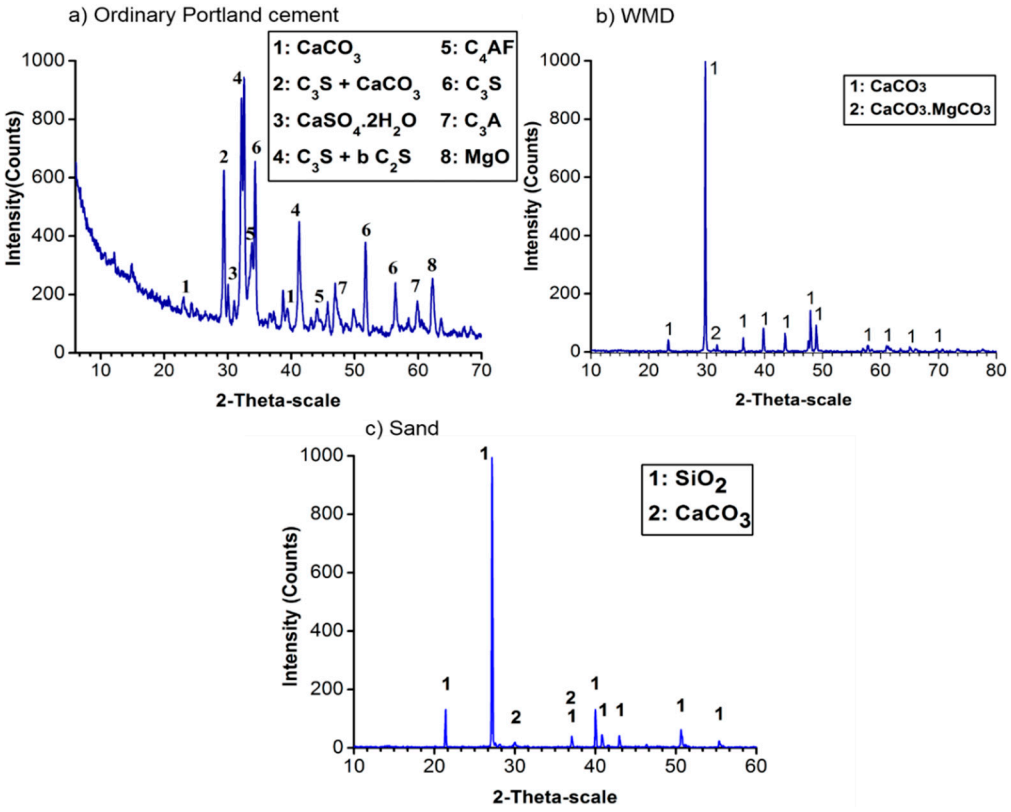

Figure 2. X-ray diffraction (XRD) spectrum of: (**a**) ordinary Portland cement; (**b**) waste marble dust (WMD); (**c**) sand.

Figure 3 presents the particle size distributions of WMD that determined using a Malvern Mastersizer 2000 analyzer (liquid: Hydro 2000MU). According to this figure, the particles in WMD smaller than 80 µm, 30 µm and 5 µm represent about 90%, 50% and 10% of the total material volume, respectively [10].

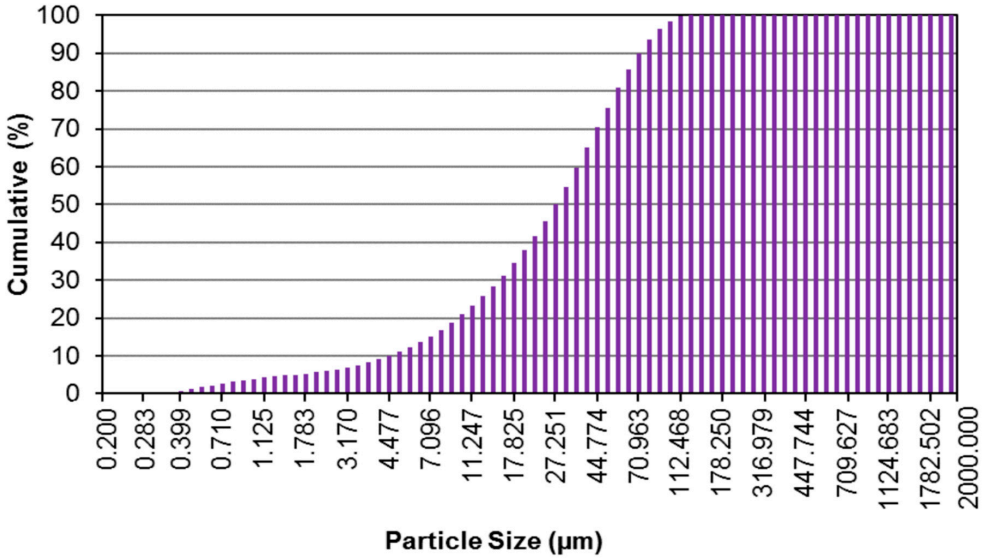

Figure 3. Particle size distribution of WMD.

2.2. Methods

As a partial replacement of the ordinary Portland cement, WMD was used. The replacement levels were 0%, 5%, 10% and 15% by weight of the cement in the mortar. The proportion of the mortar mixtures is shown in Table 2. The mortar mixtures were manufactured with a 3:1 (by mass) sand to cement ratio in accordance with the standard EN 196-1 [31]. The constant 0.5 water to binder ratio was assured according to ASTM C270-14a [32]. The flow test was repeated 3 times for each replacement ratio and determined using the following formula:

$$E\% = 100\frac{D_f - D_i}{D_i} \quad (1)$$

where:

E: Flow expressed as a percentage (%),
D_f: Final diameter (cm),
D_i: Initial diameter (cm).

Table 2. Proportions of mortar mixtures.

WMD Content (%)	Ordinary Portland Cement (kg/m^3)	WMD (kg/m^3)	Sand (kg/m^3)	Water (kg/m^3)	w/b
0	450	0	1350	225	0.5
5	427.5	22.5			
10	405	45			
15	382.5	67.5			

After determining the flow value for each sample, three prisms with dimensions of 40 × 40 × 160 mm, and three cubes of 50 mm for each replacement ratio, were prepared and then packed to avoid water evaporation. They were then put to cure in standard laboratory conditions

at 22 ± 2 °C and a relative humidity of 20 ± 1%. After 24 h, the samples were demolded and left to cure in a standard laboratory with the same conditions. Different tests were performed, such as, apparent density and compressive strength at 3 days, 7 days, 28 days, and 65 days and scanning electron microscopy analysis after 28 of being cured in standard laboratory.

The apparent density was determined according to Kirgiz [33], and the compressive strength was determined according to ASTM C 109/C109 M-9 [34]. Three cubes of 50 mm for each replacement ratio were prepared to measure the average.

The apparent density was determined using the following formula:

$$\gamma_{ad} = \frac{m_d}{v_t} \quad (2)$$

where:

γ_{ad}: Apparent density (kg/m^3),
m_d: Mass of the dry specimen (kg),
v_t: Total volume of the specimen (m^3).

The compressive strength was determined using the following formula:

$$f_{cd} = \frac{F}{A} \quad (3)$$

where:

f_{cd}: Compressive strength (MPa),
F: Failure load (N),
A: Loading area (mm^2).

The scanning electron microscopy analysis was performed after 28 of being cured in standard laboratory on samples extracted from the mid-prisms. These samples were cold-mounted in an epoxy resin and they were wet grinded using abrasive papers to make them flat. After grinding, the samples were polished with diamond paste (with dimensions of 6μm and 1μm). The cleaned samples were covered with a conductive path made of copper tape and they were then carbon coated to obtain electrical conductivity and to prevent electrical charging of the samples. A conductive layer with a thickness of 30 nm was applied in a vacuum of 1.3×10^{-4} Pa (10^{-6} Torr) with the use of the thermal evaporation method and by using sharpened graphite rods [10]. Finally, the samples can be analyzed using scanning electron microscopy to determine their microstructural properties. The JEOL JSM-6610A microscope with JED-2300 energy-dispersive X-ray spectroscopy (EDX) detector were used.

3. Results and Discussion

3.1. Properties of Fresh Mortars

The flow of mortars containing WMD is presented in Table 3.

Table 3. Flow of mortars containing WMD.

WMD Content (%)	Flow (%)	Flow Required by ASTM C270
0	110.92	110 ± 5%
5	110.90	
10	108.72	
15	107.62	

Based on the results, it can be stated that with the increase of content, the mortar flow was slightly decreased. The use of WMD in amounts of 5%, 10%, and 15% led to a decrease in the flow by 0.02%,

1.98%, and 2.96% respectively. Due to the small scale of the phenomenon, this decline may be neglected. The results were found to be in the range from 105% to 115%, which complies with ASTM C270-14a [32]. Regarding concrete, a similar observation was noticed in [26]. The authors deduced that the utilization of WMD with a lower fineness does not affect workability. On the other hand, according to [18], the utilization of WMD with a higher fineness in the manufacturing of concrete causes a decrease of workability and an increase of friction.

3.2. Properties of Hardened Mortars

In this article, the effects of the utilization of WMD on the properties of hardened ACM were considered. The compressive strength (f_{cd}) and apparent density (Υ_{ad}) of ACM were studied. Figures 4 and 5 present the obtained results of the macroscopic properties at varied curing ages.

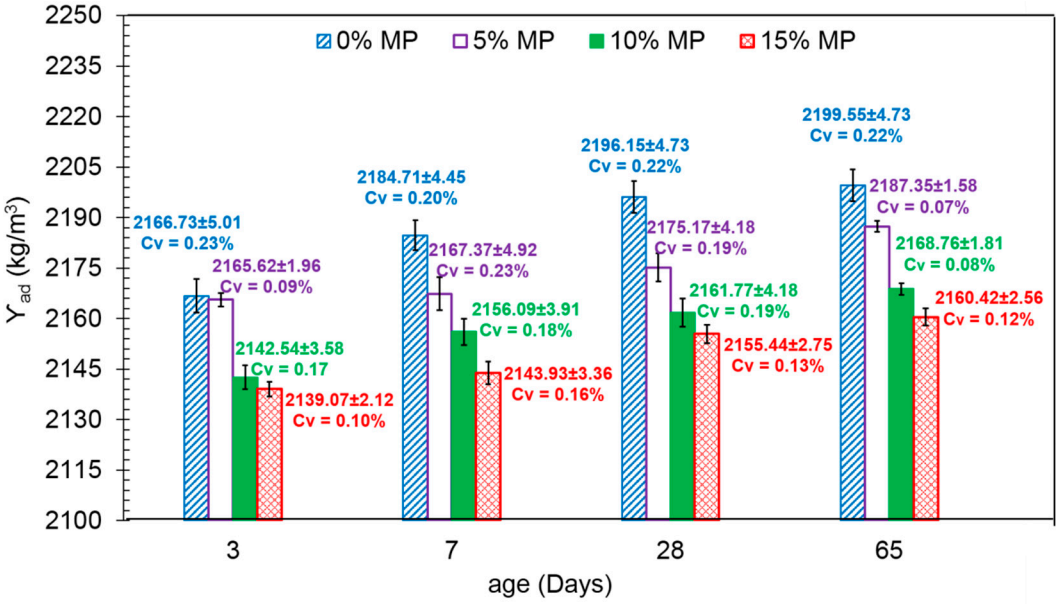

Figure 4. Apparent density of air-cured mortar (ACM) with WMD.

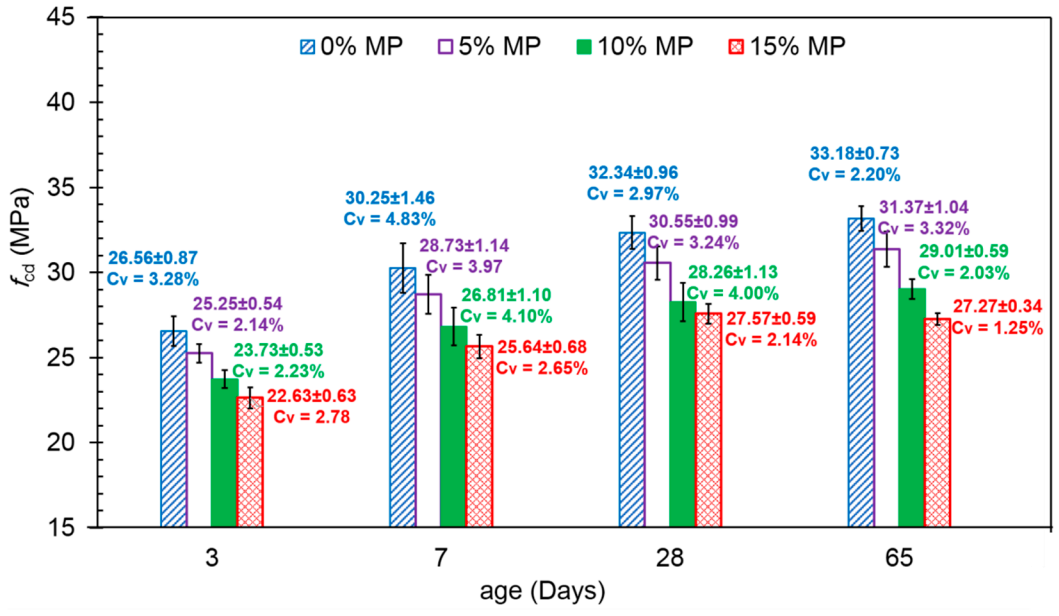

Figure 5. Compressive strength of ACM containing WMD.

As shown in Figure 4, by increasing the WMD content at all curing ages, apparent density slightly decreases when compared to the control mortar. The utilization of WMD in the amount ranging from 5% to 15% causes a decrease of the apparent density from 0.30% to 2.01% at all curing ages. This could be caused by the solid density of the WMD, which is lower than that of the ordinary Portland cement [23,25,35], and also by the inherence of ultrafine particles [10]. In addition, due to the storing of samples in air, which causes the evaporation of water, there is an incomplete hydration process and thus a decrease in the apparent density. Nevertheless, the loss in apparent density of the ACM was indiscernible [25,27] and, therefore, omitted. A contrary remarks were found in [36]. The authors indicated that the utilization of WMD as addition to the mortar causes enhancement of density. They attributed that to the density of the WMD which is greater than the density of the mortar.

Figure 5 presents the compressive strength development of the ACM with WMD. With the increase of the WMD content up to 15%, compressive strength decreases due to a lack of participation in the hydration process [37].

The utilization of WMD in amounts of 5%, 10% and 15% led to a decrease in the compressive strength at 3 days by 4.95%, 10.66% and 14.81%; at 7 days by 5.03%, 11.37% and 15.23%; at 28 days by 5.53%, 12.63% and 14.75%; and at 65 days by 5.44%, 12.56% and 17.81%, respectively.

The decrease in compressive strength proves that the presence of WMD, which does not have pozzolanic properties, reduces the effectiveness of the hydration process [29,38]. The air-curing conditions that caused water evaporation and thus created voids and internal cracks [39], as well as the decrease of apparent density and the significant reduction of the clinker content of the mixture [30], may explain the fall in compressive strength.

Microstructural details of ACM with WMD in amounts of 0%, 5%, 10% and 15% were obtained using scanning electron microscopy analysis. The backscattered electron images (BSE) were gained from mortars cured for 28 days in air conditions (Figure 6). Each particle in the images were defined using SEM–EDX analysis as illustrated in Figure 7. In addition, the compositions for each ACM containing 0%, 5%, 10%, and 15% of WMD were also determined according to grayscale. The brightness histogram of the back-scattered electron images of ACM was determined using ImageJ software, the histograms are also illustrated in Figure 6.

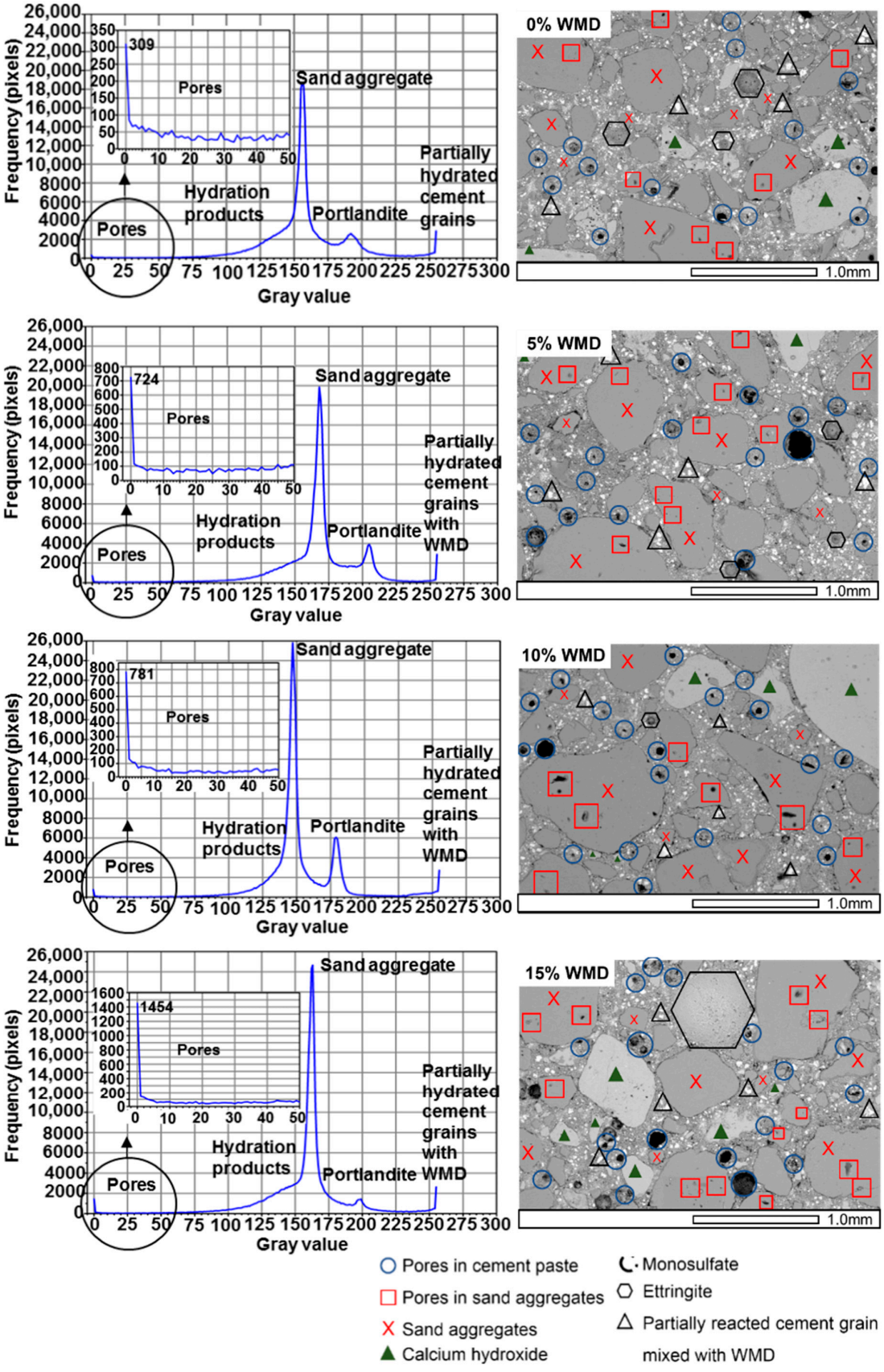

Figure 6. Back-scattered electron images and brightness histogram of ACM with various amounts of WMD.

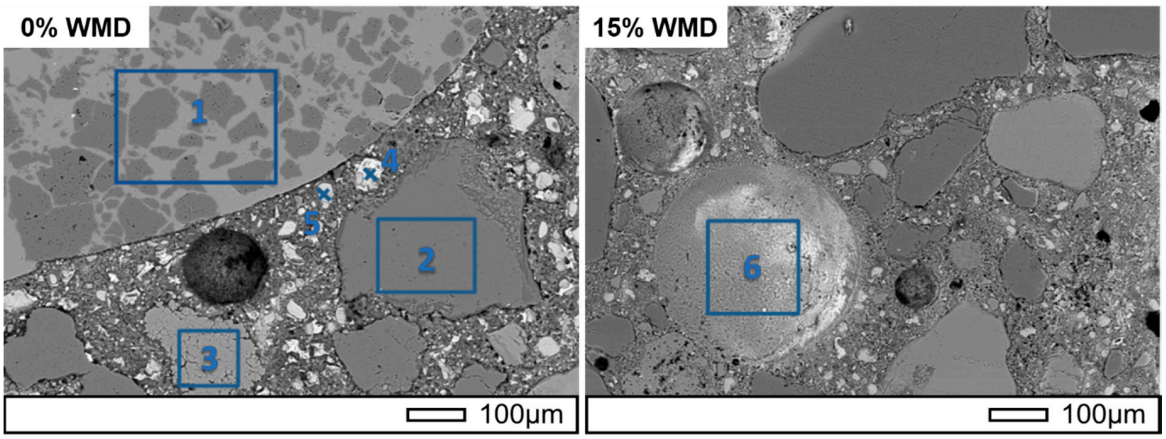

Analysis area	%O	%Ca	%Si	%Al	%Mg	%Fe
1	57.02	34.12	-	-	8.86	-
2	51.00	-	49.00	-	-	-
3	56.98	42.30	0.72	-	-	-
4	13.00	4842	1.45	1.32	1.20	34.61
5	42.34	4313	11.98	1.48	1.07	-
6	57.08	34.86	7.13	0.94	-	-

Figure 7. Scanning electron microscopy–energy-dispersive X-ray spectroscopy (SEM–EDX) analysis of ACM containing 0% and 15% WMD.

Figure 6 shows the microstructure differences of the ACM. As can be seen the ACM with WMD has a higher content of calcium hydroxide (CH). When analyzing the images, it can be seen that adding WMD to cement mortars causes higher porosity in comparison to the control mortar. This could be explained by water accumulating around WMD particles which leads to reduce the water required for the hydration of cement and, therefore, resulting in an increase in the porosity. As can be seen from the mortars containing WMD, the WMD does not appear in the images and the ettringite is too big compared to that of control mortar. This is could be explained by the reaction of calcite provided by WMD with tricalcium aluminate, which led to the formation of calcium carbo-aluminates [1,21,40]. This new chemical element is introduced in the formation of Ettringite that is why the WMD does not appear in the images and the ettringite is too big. This is confirmed by the SEM–EDX analysis of the samples with 15% WMD and without WMD (Seen Figure 7). The ettringite of the mortar containing 15% WMD appears big than that of control mortar.

As can also be seen from Figure 6, the brightness histogram for each ACM consists of five distinct peaks representing: pores, sand aggregates, hydration products, portlandite and partially hydrated cement grains. By comparison, the highest peak of pores, portlandite and partially hydrated cement grains, and lowest peak of hydration products are appeared in the ACM containing WMD, except the portlandite peak of ACM containing 15% of WMD is the lowest. In addition, there is no visible WMD peak apparently due to two reasons, the WMD is mixed and adherent with the partially hydrated cement grains and the calcite provided by WMD reacted with tricalcium aluminate which led to the formation of calcium carbo-aluminates [1,22,40]; however, the peak of hydration products appeared lower in the ACM containing WMD. This is due to a decrease of C-S-H content, this content representing between 50–70% of the hydrated products.

The pores content and the percentage of the calcium hydroxide (CH) could be determined based on BSE images and chemical mappings (Figure 8). Microcracks were avoided during the analysis.

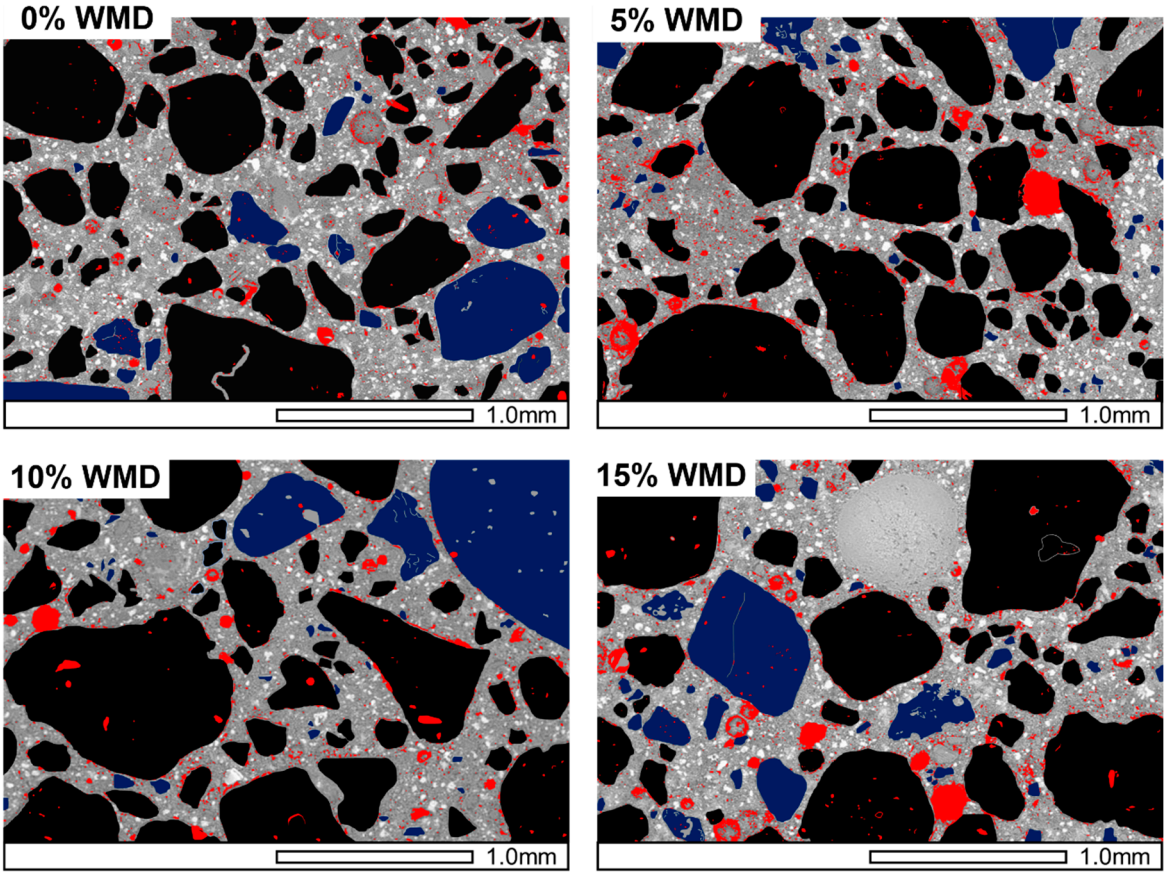

Figure 8. Scanning electron microscopy (SEM) images of ACM with WMD: calcium hydroxide (blue particles); pores (red particles); sand aggregate (black particles); partially reacted cement grain mixed with WMD (white particles); hydrate products (gray color).

When analyzing data from Figure 8, it can be noted that the increasing amounts of WMD up to 15% cause a growth in the calcium hydroxide (CH) content. In addition, it can also be seen from this figure that the porosity increases with a corresponding increase in the amounts of WMD up to 15%. This could be explained by the trapped air that formed when ordinary Portland cement and sand aggregates are mixed with WMD. They cannot be easily removed because the air tends to be stabilized by WMD. Table 4 presents the porosity and CH results.

Table 4. Area and percentage share of pores and calcium hydroxide (CH) based on the magnified scanning electron microscopy images of ACM with WMD.

WMD Content (%)	Area and Percentage Share of Pores (mm^2)			Area and Percentage Share of CH (mm^2)
	In Mortars	In Sand Aggregates	In Cement Matrix	
0	0.349 (7.739%)	0.013 (0.287%)	0.336 (7.452%)	0.378 (8.391%)
5	0.373 (8.393%)	0.013 (0.283%)	0.360 (8.110%)	0.396 (8.910%)
10	0.376 (8.513%)	0.013 (0.297%)	0.363 (8.216%)	0.402 (9.098%)
15	0.399 (8.991%)	0.012 (0.272%)	0.387 (8.719%)	0.408 (9.201%)

Considering the data in Table 4, it can be seen that the increasing amounts of WMD from 0% to 15% led to an increase in porosity and CH content from 7.739% to 8.991% and from 8.391% to 9.201%, respectively.

It is visible from Table 4 that the porosity of the cement matrix increases with corresponding increase in the amounts of WMD. This can be mainly due to the fact that the WMD can trap water (water accumulates around WMD particles). It may lead to the reduction of water required for the hydration of cement particles and therefore resulting an increase in the porosity. In addition, the WMD may accumulate around the cement grains. It can prevent the contact between the cement grains and water and therefore leads to a slight reduction of the hydration products. Finally, this reduction may contribute to an increase in porosity.

This increase in porosity also had an influence on the compressive strength [41]. The utilization of WMD in amounts of 5%, 10% and 15% led to an increase in the porosity of cement matrix in mortar at 28 days by 8.483%, 10.25% and 17.00%, respectively.

On the other hand, the CH content increased in the ACM at 28 days by 6.18%, 8.43%, and 9.65% when using WMD in amounts of 5%, 10%, and 15%, respectively. The increase in CH is accompanied by a decrease of C-S-H.

The replacement of ordinary Portland cement by WMD causes a decrease of C-S-H and an increase of CH content. It may be mainly due to the change in water distribution when the different amounts of WMD are used that leads to an incomplete hydration process. According to our previous studies [10,30], the SEM–EDX analysis indicates that the samples blended with WMD have higher Ca and lower Si content due to the $CaCO_3$ provided by WMD and lower SiO_2 found in WMD, thus the WMD contributes to the increase in the CH and decrease in the C-S-H.

Finally, the pore size distribution area in the ACM containing different amounts of WMD using ImageJ software was determined, and the results are presented in Figure 9.

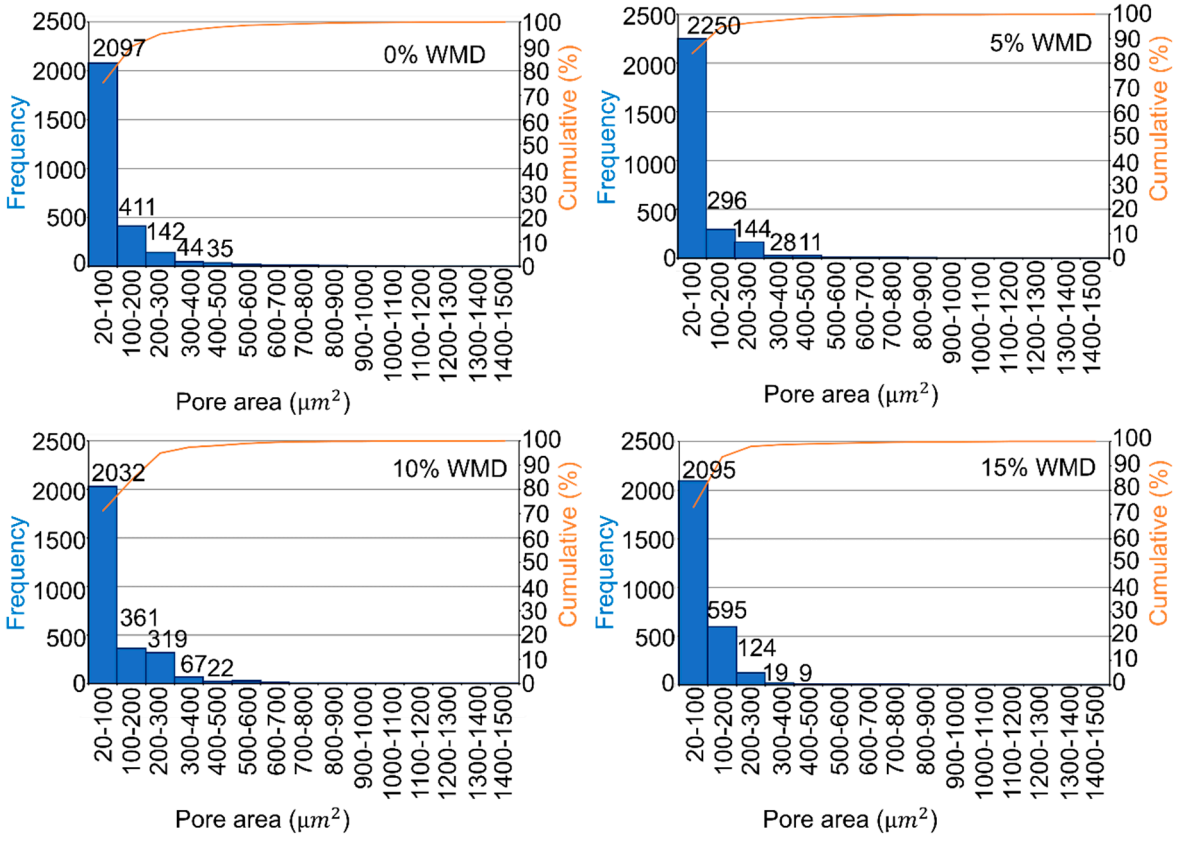

Figure 9. Pore size distribution area and cumulative of ACM containing WMD.

As can be seen from Figure 9, 97% of the pore area varied from 20 to 500 μm^2 (the pore diameter varied from 5 to 25 μm). In addition, the increase in amounts of WMD up to 15% led to an increase of pore size area in this range. It may be because 50% of the WMD particles have a size less than 30 μm and thus most of the pores smaller than 30 μm cannot be filled by WMD. These pores represent the spaces previously occupied by water.

4. Conclusions

Based on the experimental results of ACM, the following conclusions may be drawn from the work presented in this paper:

1. The utilization of WMD as a partial replacement of cement does not significantly affect the flow property of fresh mortar, where the results were found to be compatible with ASTM C270.
2. The macro properties of mortars were affected negatively due to the incorporation of WMD and to the air-curing conditions that caused an incomplete hydration process in which the compressive strength and apparent density decreased, and the porosity increased.
3. The compressive strength and apparent density of ACM mixed with and without WMD grew with an increase in curing duration and fell with a corresponding increase of WMD.
4. The use of WMD in an amount of up to 15% caused an increase in porosity. It may be mainly due to the trapped water between WMD particles which reduces the water required for the hydration of cement. In addition, the accumulated WMD around the cement grains can prevent the hydration process.
5. The utilization of WMD has trapped the air in the mortar and, thus, trapping air creates air voids.
6. The brightness histogram of ACM indicates that the utilization of WMD contributes to an increase of pores, CH and partially hydrated grains and a decrease of hydration products.
7. The CH content of the cement matrix in ACM increases with a corresponding increase of WMD. It may be mainly due to the water accumulating around WMD particles that leads to an incomplete hydration process. In addition, the WMD may accumulate around the cement grains and can prevent the contact between the cement grains and water. Therefore, it may lead to a slight reduction of the hydration products.
8. The pore area in ACM smaller than 500 μm^2 represent 97% of the total pores, and these pores represent the spaces previously occupied by water. The WMD cannot can fill these pores because 50% of its particles are less than 30 μm.

Indeed, the WMD affects negatively the properties of air-cured mortar; however, due to the low solid density of applied WMD compared to the solid density of ordinary Portland cement in construction practice, it may be economically sensible to use of WMD in lightweight cement-based materials used for non-structural elements.

Author Contributions: Conceptualization, M.M. and Ł.S.; Data curation, N.T.S., A.K. and A.Ż.; Formal analysis, M.M.; Funding acquisition, M.M.; Investigation, N.T.S.; Methodology, N.T.S. and Ł.S.; Resources, N.T.S.; Software, A.K. and A.Ż.; Supervision, M.M. and Ł.S.; Visualization, A.K. and A.Ż.; Writing—original draft, N.T.S.; Writing—review and editing, Ł.S., A.Ż. and Krzysztof Ostrowski.

Funding: This research received funding from the project no. 0401/0116/18 entitled "Non-destructive and semi-destructive methods of evaluation of the materials, elements and building structures" ["Nieniszczące i seminiszczące metody badania materiałów, elementów i konstrukcji budowlanych"] funded by the Ministry of Science and Higher Education in Poland.

Acknowledgments: The authors would like to acknowledge the support of the Electron Microscopy Laboratory at Wroclaw University of Science and Technology in Poland for enabling the scanning electron microscopy analysis to be performed.

Conflicts of Interest: The authors declare no conflict of interest.

References

1. Arel, H.Ş. Recyclability of waste marble in concrete production. *J. Clean. Prod.* **2016**, *131*, 179–188. [CrossRef]
2. Siddique, R. Performance characteristics of high-volume Class F fly ash concrete. *Cem. Concr. Res.* **2004**, *34*, 487–493. [CrossRef]
3. Stajanča, M.; Eštoková, A. *Environmental Impacts of Cement Production*; University of Košice: Košice, Slovakia, 2012.
4. Kurad, R.; Silvestre, J.D.; de Brito, J.; Ahmed, H. Effect of incorporation of high volume of recycled concrete aggregates and fly ash on the strength and global warming potential of concrete. *J. Clean. Prod.* **2017**, *166*, 485–502. [CrossRef]
5. Aruntaş, H.Y.; Gürü, M.; Dayı, M.; Tekin, I. Utilization of waste marble dust as an additive in cement production. *Mater. Des.* **2010**, *31*, 4039–4042. [CrossRef]
6. Andrew, R.M. Global CO_2 emissions from cement production. *Earth Syst. Sci. Data* **2018**, *10*, 195. [CrossRef]
7. Worrell, E.; Price, L.; Martin, N.; Hendriks, C.; Meida, L.O. Carbon dioxide emissions from the global cement industry. *Annu. Rev. Energy Environ.* **2001**, *26*, 303–329. [CrossRef]
8. Alyousef, R.; Khadimallah, M.A.; Soussi, C.; Benjeddou, O.; Jedidi, M. Experimental and Theoretical Study of a New Technique for Mixing Self-Compacting Concrete with Marble Sludge Grout. *Adv. Civ. Eng.* **2018**, 1–11. [CrossRef]
9. Nežerka, V.; Hrbek, V.; Prošek, Z.; Somr, M.; Tesárek, P.; Fládr, J. Micromechanical characterization and modeling of cement pastes containing waste marble powder. *J. Clean. Prod.* **2018**, *195*, 1081–1090. [CrossRef]
10. Toubal Seghir, N.; Mellas, M.; Sadowski, Ł.; Żak, A. Effects of marble powder on the properties of the air-cured blended cement paste. *J. Clean. Prod.* **2018**, *183*, 858–868. [CrossRef]
11. Nagrockienė, D.; Girskas, G.; Skripkiūnas, G. Properties of concrete modified with mineral additives. *Constr. Build. Mater.* **2015**, *135*, 37–42. [CrossRef]
12. Su, H.; Jing, H.; Yin, Q.; Yu, L. Effect of Thermal Environment on the Mechanical Behaviors of Building Marble. *Adv. Civ. Eng.* **2018**, 1–8. [CrossRef]
13. Hebhoub, H.; Aoun, H.; Belachia, M.; Houari, H.; Ghorbel, E. Use of waste marble aggregates in concrete. *Constr. Build. Mater.* **2011**, *25*, 1167–1171. [CrossRef]
14. Uysal, M. The Use of Waste Maroon Marble Powder and Iron Oxide Pigment in the Production of Coloured Self-Compacting Concrete. *Adv. Civ. Eng.* **2018**, 1–10. [CrossRef]
15. Celik, M.Y.; Sabah, E. Geological and technical characterisation of Iscehisar (Afyon-Turkey) marble deposits and the impact of marble waste on environmental pollution. *J. Environ. Manag.* **2008**, *87*, 106–116. [CrossRef]
16. Saha, A.K.; Sarker, P.K. Compressive strength of mortar containing ferronickel slag as replacement of natural sand. *Procedia Eng.* **2017**, *171*, 689–694. [CrossRef]
17. Aliabdo, A.A.; Abd Elmoaty, A.E.M.; Auda, E.M. Re-use of waste marble dust in the production of cement and concrete. *Constr. Build. Mater.* **2014**, *50*, 28–41. [CrossRef]
18. Ashish, D.K.; Verma, S.K.; Kumar, R.; Sharma, N. Properties of concrete incorporating sand and cement with waste marble powder. *Adv. Concr. Construct.* **2016**, *4*, 145–160. [CrossRef]
19. Boukhelkhal, A.; Azzouz, L.; Salah, A.; Belaïdi, E. Effects of marble powder as a partial replacement of cement on some engineering properties of self- compacting concrete. *J. Adhes. Sci. Technol.* **2016**, *30*, 2405–2419. [CrossRef]
20. Corinaldesi, V.; Moriconi, G.; Naik, T.R. Characterization of marble powder for its use in mortar and concrete. *Constr. Build. Mater.* **2010**, *24*, 113–117. [CrossRef]
21. Ergün, A. Effects of the usage of diatomite and waste marble powder as partial replacement of cement on the mechanical properties of concrete. *Constr. Build. Mater.* **2011**, *25*, 806–812. [CrossRef]
22. Gesoğlu, M.; Güneyisi, E.; Kocabag, M.E.; Bayram, V.; Mermerdaş, K. Fresh and hardened characteristics of self compacting concretes made with combined use of marble powder, limestone filler, and fly ash. *Constr. Build. Mater.* **2012**, *37*, 160–170. [CrossRef]
23. Mashaly, A.O.; El-Kaliouby, B.A.; Shalaby, B.N.; El–Gohary, A.M.; Rashwan, M.A. Effects of marble sludge incorporation on the properties of cement composites and concrete paving blocks. *J. Clean. Prod.* **2016**, *112*, 731–741. [CrossRef]
24. Rana, A.; Kalla, P.; Csetenyi, L.J. Sustainable use of marble slurry in concrete. *J. Clean. Prod.* **2015**, *94*, 304–311. [CrossRef]

25. Rodrigues, R.; De Brito, J.; Sardinha, M. Mechanical properties of structural concrete containing very fine aggregates from marble cutting sludge. *Constr. Build. Mater.* **2015**, *77*, 349–356. [CrossRef]
26. Sardinha, M.; De Brito, J.; Rodrigues, R. Durability properties of structural concrete containing very fine aggregates of marble sludge. *Constr. Build. Mater.* **2016**, *119*, 45–52. [CrossRef]
27. Singh, M.; Srivastava, A.; Bhunia, D. Long term strength and durability parameters of hardened concrete on partially replacing cement by dried waste marble powder slurry. *Constr. Build. Mater.* **2019**, *198*, 553–569. [CrossRef]
28. Talah, A.; Kharchi, F.; Chaid, R. Influence of Marble Powder on High Performance Concrete Behavior. *Procedia Eng.* **2015**, *114*, 685–690. [CrossRef]
29. Vardhan, K.; Siddique, R.; Goyal, S. Strength, permeation and micro-structural characteristics of concrete incorporating waste marble. *Constr. Build. Mater.* **2019**, *203*, 45–55. [CrossRef]
30. Toubal Seghir, N.; Mellas, M.; Sadowski, Ł.; Krolicka, A.; Żak, A. The Effect of Curing Conditions on the Properties of Cement-Based Composites Blended with Waste Marble Dust. *JOM* **2019**, *71*, 1002–1015. [CrossRef]
31. Standard Methods of Testing Cement. Determination of Strength. Available online: https://www.thenbs.com/PublicationIndex/documents/details?Pub=BSI&DocID=274735 (accessed on 12 April 2019).
32. ASTM C270-14a. Standard specification for mortar for unit masonry. In *Annual Book of ASTM Standards 4*; ASTM Standards: West Conshohocken, PA, USA, 2003.
33. Kirgiz, M.S. Advancements in mechanical and physical properties for marble powder–cement composites strengthened by nanostructured graphite particles. *Mech. Mater.* **2016**, *92*, 223–234. [CrossRef]
34. ASTM C109/C109 M-99. Standard test method for the compressive strength of hydraulic cement mortars (using 2-in. or [50-mm] cube specimens). In *Annual Book of ASTM Standards 4*; ASTM Standards: West Conshohocken, PA, USA, 1999.
35. Gencel, O.; Ozel, C.; Koksal, F.; Erdogmus, E.; Martínez-Barrera, G.; Brostow, W. Properties of concrete paving blocks made with waste marble. *J. Clean. Prod.* **2012**, *21*, 62–70. [CrossRef]
36. Buyuksagis, I.S.; Uygunoglu, T.; Tatar, E. Investigation on the usage of waste marble powder in cement-based adhesive mortar. *Constr. Build. Mater.* **2017**, *154*, 734–742. [CrossRef]
37. Alyousef, R.; Benjeddou, O.; Khadimallah, M.A.; Mohamed, A.M.; Soussi, C. Study of the Effects of Marble Powder Amount on the Self-Compacting Concretes Properties by Microstructure Analysis on Cement-Marble Powder Pastes. *Adv. Civ. Eng.* **2018**, 1–13. [CrossRef]
38. Khyaliya, R.K.; Kabeer, K.I.S.A.; Vyas, A.K. Evaluation of strength and durability of lean mortar mixes containing marble waste. *Constr. Build. Mater.* **2017**, *147*, 598–607. [CrossRef]
39. Saha, A.K.; Sarker, P.K.; Majhi, S. Effect of elevated temperatures on concrete incorporating ferronickel slag as fine aggregate. *Fire Mater.* **2019**, *43*, 8–21. [CrossRef]
40. Ulubeyli, G.C.; Artir, R. Properties of Hardened Concrete Produced by Waste Marble Powder. *Procedia Soc. Behav. Sci.* **2015**, *195*, 2181–2190.
41. Liu, D.; Šavija, B.; Smith, G.E.; Flewitt, P.E.; Lowe, T.; Schlangen, E. Towards understanding the influence of porosity on mechanical and fracture behaviour of quasi-brittle materials: Experiments and modelling. *Int. J. Fract.* **2017**, *205*, 57–72. [CrossRef]